Corrosion behaviour of Mg alloys cladding from nuclear reactors fuel in alkaline solutions

J. Agullo, B. Muzeau, Christian Bataillon, V. l'Hostis

Corrosion behaviour of Mg alloys cladding from nuclear reactors fuel in alkaline solutions

J. Agullo, B. Muzeau, C. Bataillon, V. L'Hostis, CEA Saclay, Gif-sur-Yvette/France

Summary

The reprocessing of spent fuel from the French UNGG (Graphite Gas Natural Uranium) nuclear power plants generates cladding wastes such are Mg-Mn alloys. A storage strategy is to encapsulate these wastes into cement matrix. The main issue is hydrogen evolution as the main consequence of the corrosion of Mg alloys, regardless of concrete radiolysis. In fact Mg acts as an anode in most of galvanic corrosion systems and the hydrogen can be produced either by water reduction or by Anodic Hydrogen Evolution (AHE). In the last case, an increase in the rate of hydrogen production with increasing applied potential is observed. This phenomenon called "Negative Different Effect" (NDE) is in contradiction with the conventional Tafel equation. The corrosion of magnesium may produce Mg^{+} cations which react quickly with water to produce hydrogen and stable Mg^{2+} cations.

The interstitial solution in concrete pores is characterized by a very high pH. To reproduce the pH solution around 13, 0.1M NaOH solutions were prepared and used as electrolytes from electrochemical experiments. Stainless steel, platinum and graphite were used as cathode to investigate basic galvanic coupling as it can be encountered in the real wastes.

The purpose of this work was to investigate the galvanic corrosion of Mg alloys in the high pH solutions. The study of Mg corrosion behaviour was carried out using electrochemical measurement: ZRA mode. The analysis of the surface and the corrosion products were performed by Raman spectroscopy. The first results showed a galvanic corrosion rate more important with stainless steel rather than with graphite.

1 Introduction

The reprocessing of spent fuel from the French UNGG (Graphite Gas Natural Uranium) nuclear power plants generates decanning wastes. Cladding wastes are made of metal uranium rod sheathed with magnesium alloys. Two types can be distinguished: the body cladding of the assembly with Mg-0.8wt.%Zr and the two exhaust caps with Mg-wt.1.2%Mn. The packaging of these wastes considered so far is based on their immobilization in an hydraulic binder. Several have been tested (RHEOMAC, white OPC, white OPC with blast furnace slag, fly ash cement, C_3S, Geopolymer, etc.., in paste or mortar) [1-5]. In all cases, they imply that the wastes are exposed to a highly alkaline environment (pH> 12) and subjected to heat of hydration. Some Mg alloy decanning wastes could be into direct contact with graphite from the fuel assemblies or steel from the container leading to an electrical coupling. The presence of an electrolyte, like the interstitial solution of the cement matrix, allows the realization of an electrical circuit involving galvanic corrosion phenomena [5]. Since Mg acts as an anode in most of galvanic corrosion systems its corrosion rate will be accelerated. In

fact thermodynamically Mg is very reactive with a normal potential of -2.36 V/NHE (Normal Hydrogen Electrode) [6]. An E-pH diagram can predicted the thermodynamic stability or tendency for corrosion of Mg in water.

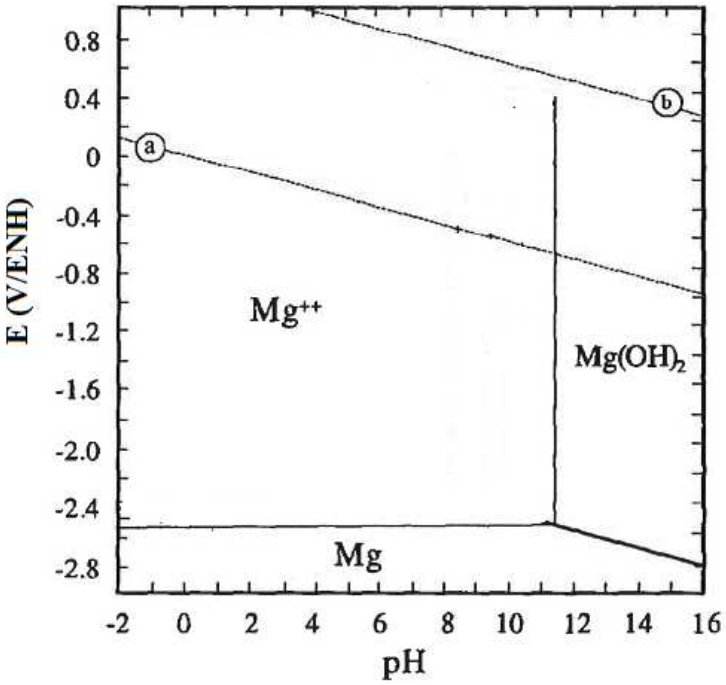

Figure 1: E-pH diagram of Mg in aqueous solution at 25 °C.
The lines a and b identify the reaction of hydrogen and oxygen evolution, respectively [7].

In alkaline media the different reaction at the equilibrium potential are the following:

Anodic reaction: $Mg \rightarrow Mg^{2+} + 2e^-$ (eq. 1)

Chemical reaction: $Mg^{2+} + 2HO^- \rightarrow Mg(OH)_2$ (eq. 2)

Cathodic reaction: $2H_2O + 2e^- \rightarrow H_2 + 2HO^-$ (eq. 3)

Overall reaction: $Mg + 2H_2O \rightarrow Mg(OH)_2 + H_2$ (eq. 4)

Unfortunately in the Mg case thermodynamic data cannot effectively predict phenomena that come into play during its corrosion. It must take into account all the kinetic aspects which are determinant in Mg corrosion behaviour [8].

The anodic process of Mg is still in discussion because it exhibits behaviour in contradiction with the conventional Tafel equation. In fact, an increase in the rate of hydrogen production with increasing applied potential is observed. This phenomenon is called “Negative Different Effect” (NDE) [9]. A hypothesis proposes that the corrosion of magnesium may produce Mg^+ cations (eq. 5) which react quickly with water to produce hydrogen and stable Mg^{2+} cations (eq. 6).

Anodic reaction: $Mg \rightarrow Mg^+ + e^-$ (eq. 5)

Chemical reaction: $Mg^+ + H_2O \rightarrow Mg^{2+} + 1/2H_2 + HO^-$ (eq. 6)

Concerning the cathodic process, oxygen reduction and hydrogen evolution should be considered in basic media. However in the case of Mg dissolved oxygen does not play an important role and hydrogen evolution is the main cathodic process (eq. 3).

It appears that hydrogen evolution can be produced either by water reduction (eq.3) or by Anodic Hydrogen Evolution (AHE, eq. 6). Galvanic coupling of Mg acting as an anode could involve a rapid evolution of hydrogen and corrosion of Mg. The main issue is hydrogen evolution as the main consequence of the corrosion of Mg alloys, regardless of concrete radiolysis. Uncontrolled hydrogen production could have deleterious consequences for the package, such as cracking of the embedding matrix and increase the risk of fire in the storage area. The other issue is the accumulation of solid corrosion products which could cause the development of sufficient expansive force to deform the waste containers [5]. According to the E-pH diagram in alkaline media and due to dissolution of Mg and hydrogen evolution, the Mg surface becomes more alkaline than the bulk solution involving a deposit of $Mg(OH)_2$ on the surface.

The purpose of this work was to investigate the galvanic corrosion of Mg alloys in the high pH solutions with platinum, graphite and stainless steel 304L. Platinum was chosen as noble metal, graphite is present in the wastes and stainless steel 304L may also be found in the wastes. The study of Mg corrosion behaviour was carried out using electrochemical measurement: ZRA measurement. The analysis of the surface and the corrosion products were performed by Raman spectroscopy.

2 Materials and experimental

Galvanic corrosion was achieved by coupling the pairs of metals together via a Zero Resistance Ammeter (ZRA). The galvanic current of the coupled metal was measured over time. Electrochemical measurements were carried out at room temperature in a flat cell provided by Gamry Instruments in a three-electrode configuration with a Gamry PCI4/300 potentiostat. An Hg/HgO (0.1M NaOH) reference electrode (E° = 0.165 V/NHE) was used for all experiments in 0.1M NaOH for electrolyte. A nominal area of 2.6 cm^2 defined by the Gamry Flatcell setup were exposed to the solution. The anode electrode consisted of Mg-Mn alloy (Mg 99.2wt.% and Mn 0.8wt.%). The cathode was constituted of a platinum gauze (>99.99%, Alfa Aesar), graphite from the G2 reactor (French UNGG reactor) or stainless steel 304L. The Mg-Mn surface was cleaned by polishing with ethanol on SiC Grinding paper in different roughness between 180 to 800 grit (Struers). Then, the electrode was rinsed with ethanol and dried with KIMTECH brand wipers and stored in desiccator in the presence of silica gel. All solutions were prepared using Mili-Q deionized water (ρ > 18.2 $M\Omega.cm^{-1}$) and all the experiments were carried out at a room temperature.
Raman spectra were recorded with an X'plora Raman spectrometer (Horiba-Jobin Yvon) using a laser at λ = 532 nm and a 600 lines/mm grating.

2 Results and discussion

1 Influence of the stabilization of the electrochemical system with galvanic coupling

The first system investigated is composed of an Mg alloy anode and a platinum cathode electrode with an Hg/HgO (NaOH 0,1M) reference electrode. Platinum was chosen initially for guidance because it is a noble metal that has a well-documented behaviour. The goal of this section is to estimate the influence of the stabilization system on its final state. Several sequences were performed by varying the time of stabilization of the electrochemical cell before performing a galvanic coupling. The corrosion potential noted Ecorr was recorded for 0, 1 or 18h before switching to ZRA mode.

- Sequence 1: corrosion potential of 18h followed by a ZRA mode
- Sequence 2: corrosion potential 1h followed by a ZRA mode
- Sequence 3: direct ZRA mode

In the first two phases, the corrosion potential increases after 5 min of balance (see Figures 2 and 4). When galvanic coupling occurs, regardless of the stabilization time, a transient from 2 to 3000 seconds is observed (see Figures 3, 5 and 6). This regime reflects the start-up of the system. Generally during the experiment, when the current values decrease, potential values increase. This indicates a cathodic Butler-Volmer relationship, suggesting a cathodic control. The values of current density and potential after the arbitrary value of 60 000 s (16h40) in ZRA mode are very close, about 0.134 V/NHE and 1.16 µA.cm^{-2}. The system tends to the same final state. The same observations were made for Mg alloy systems coupled with graphite or 304L. The curves obtained have shown good reproducibility for the different sequences and different couplings.

Subsequently, it was decided to impose a galvanic coupling system without stabilization. This cannot change the state of the electrode surface before the galvanic coupling and it is more representative of reality as contacts exist in the waste packages.

Sequence 1

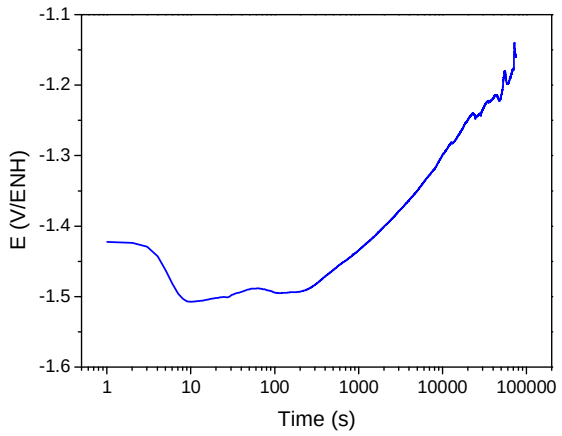

Figure 2: Potential values of Mg alloy as a function of time in 0.1M NaOH.

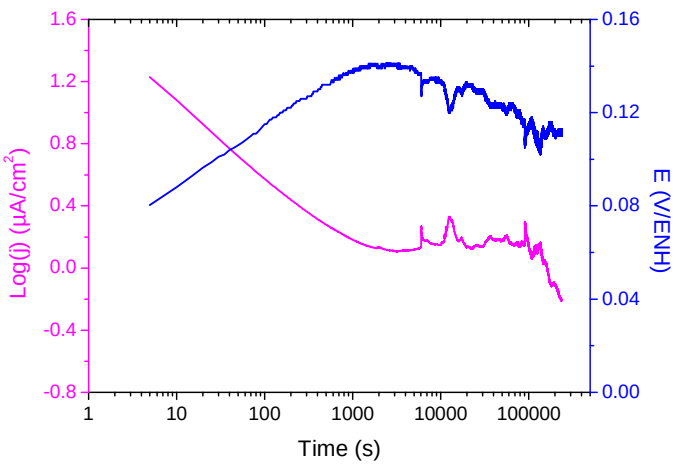

Figure 3: Potential and galvanic density current values as a function of time for Mg alloy coupled with Pt, in ZRA mode after 18h of stabilization in 0.1M NaOH.

Sequence 2	
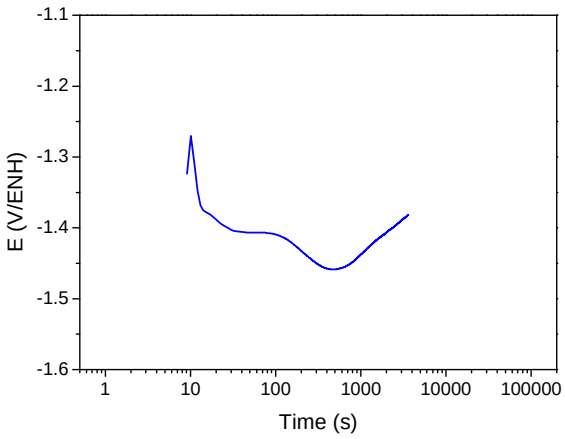	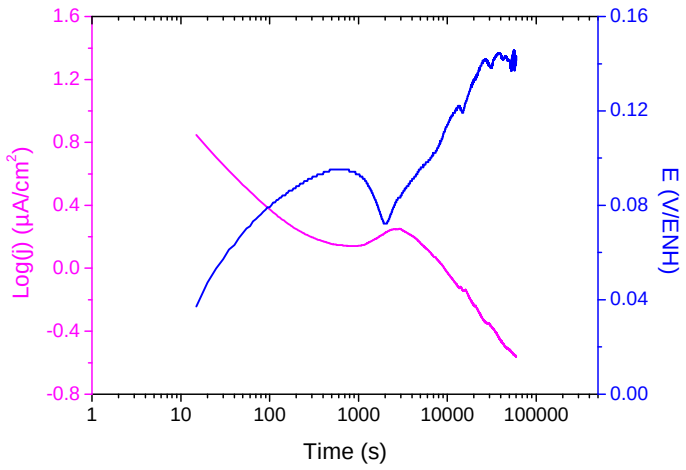
Figure 4: Potential values of Mg alloy as a function of time in 0.1M NaOH.	**Figure 5:** Potential and galvanic density current values as a function of time for Mg alloy coupled with Pt, in ZRA mode after 1h of stabilization in 0.1M NaOH.

Sequence 3
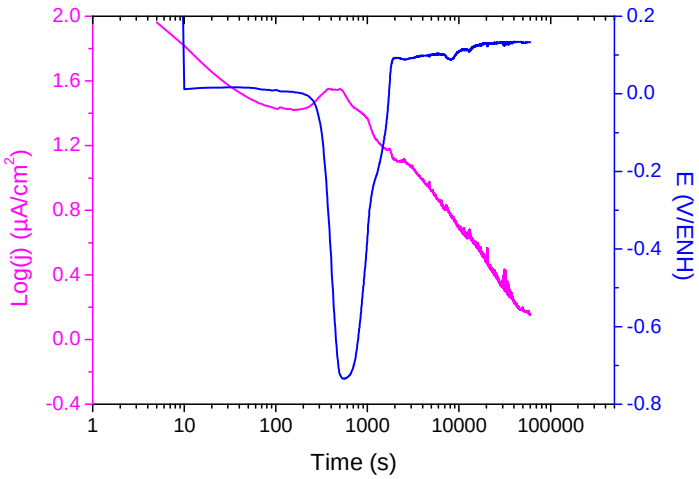
Figure 6: Potential and galvanic density current values as a function of time for Mg alloy coupled with Pt, in ZRA mode without stabilization in 0.1M NaOH.

2 Influence of the galvanic coupled material in the corrosion of magnesium in aqueous media

The Figure 7 represents the galvanic density current values and the potential as a function of time for Mg alloy coupled with Pt, graphite or 304L in ZRA mode after transient regime.

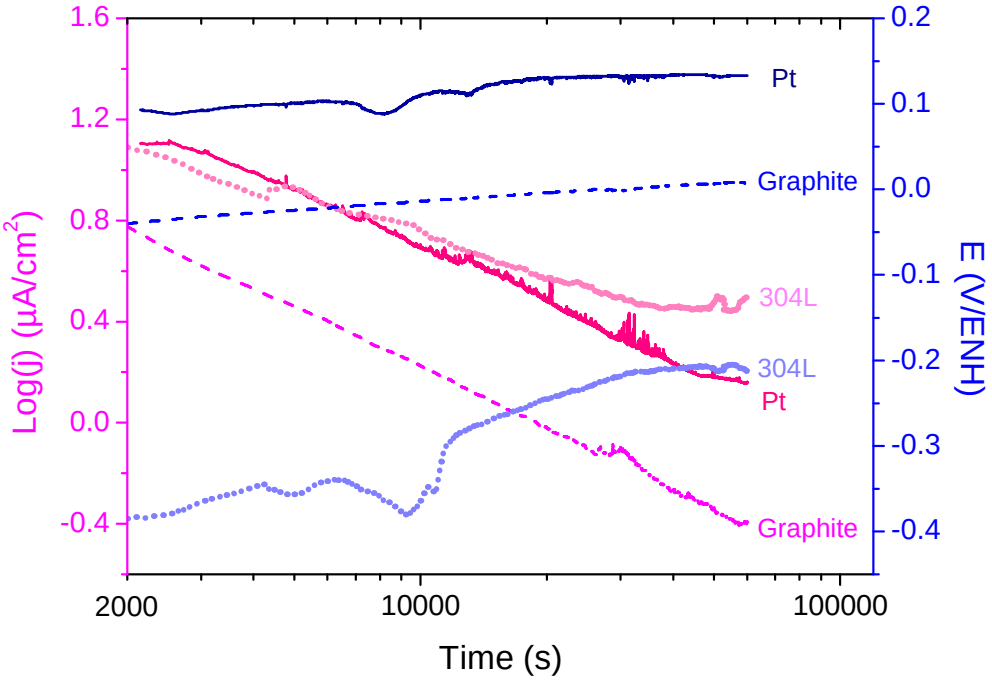

Figure 7: Potential and galvanic density current values as a function of time for Mg alloy coupled with Pt, graphite or 304L in ZRA mode after transient regime.

In our experimental conditions (anode/cathode area=1), galvanic coupling is under cathodic control. For each couple when current values decrease potential values increase. The potential values vary with the cathode, in ascending order for 304L, graphite and platinum. They can be treated as straight as a first approximation. Platinum and graphite have a slope value very close and less than 304L.
The comparison of the curves obtained for the current density shows that the corrosion kinetics appears to be close to the three cathodes used.
The current values at 60 ks indicate lower current density for graphite, platinum and 304L, respectively. It was rather expected that the values of current density are higher for platinum, graphite and then to 304L. This would indicate greater corrosion kinetics of these materials in this order.

The following equations allow the calculation of the amount of H_2 that would be released and the corrosion rate in theoretical case.

$$V_{H_2} = n \cdot V_m \qquad \text{(eq. 7)}$$

with V_{H2} volume of gas formed (L), n number of moles (mol) and V_m molar volume (22.4 $L.mol^{-1}$).

Considering that 2 electrons are exchanged in the process of corrosion of magnesium, z = 2 and using the value of the molar mass of magnesium (M=24.305 $g.mol^{-1}$) and its specific mass (ρ=1.74 $g.cm^{-3}$), the relationship between the corrosion rate and the current density of corrosion is the following [2]:

$$v_{corr} = \frac{M}{z \cdot \rho \cdot F} \cdot j_{corr} \qquad \text{(eq. 8)}$$

Or

$$v_{corr} = 22.85 \cdot j_{corr} \qquad \text{(eq. 9)}$$

with j_{corr}: current density of corrosion ($A.cm^{-2}$),
v_{corr}: corrosion rate ($m.y^{-1}$).

From the values after 60 ks of galvanic coupling and equations 7 and 9, the corrosion rates and the amount of H_2 that would be released over a year can be calculated with the following assumptions:
- The solution is assumed to be uniform, j_{corr} can be likened to j_0, equilibrium current density value,
- Two electrons are exchanged in the process of corrosion of magnesium according to equation 1,
- Hydrogen evolution from the cathode reaction of only one mole of Mg and corresponds to one mole of H_2 (eq. 4)

Corrosion rates are on the order of a few tens of micrometers per year, which corresponds to the order of magnitude reported in the literature [5, 10]. However, the extrapolated values of the H_2 generated volumes are relatively high as shown in the table 1.

Table 1: Values of the current density and potential and the estimated corrosion rate of Mg alloy in galvanic coupling with platinum, graphite and 304L after 60 ks.

Couple	Values after 60 ks of ZRA			
	E_{corr} (V/ENH)	j_{corr} ($\mu A.cm^{-2}$)	corrosion rate ($\mu m.y^{-1}$)	H_2 gas formed ($L.m^{-2}.y^{-1}$)
Mg alloy/Pt	0.133	1.45	33	53
Mg alloy/Graphite	0.072	0.41	9	15
Mg alloy /304L	-0.213	3.16	72	116

3 Surface film

The figure 8 shows two samples of Mg alloy before and after galvanic coupling with graphite during 16h in 0.1M NaOH. The part of the sample in contact with the solution was delimited by O-ring and presents a yellow-brown aspect. The same observation was done for platinum and 304L.

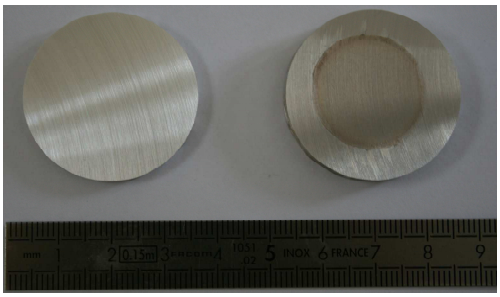

Figure 8: Mg alloy sample before (on the left) and after (on the right) galvanic coupling with graphite during 16h in 0.1M NaOH.

Brucite ($Mg(OH)_2$) is expected to be found after the galvanic corrosion of Mg alloy [8, 11]. Brucite is characterized by Raman active O-H stretching vibration around 3650 cm^{-1} [12]. Raman spectra of Mg alloys before and after galvanic corrosion with platinum, graphite and stainless steel were recorded. Similar spectra were obtained for all anodes after galvanic coupling with Mg alloy in alkaline media. Figure 9 presents the case of galvanic coupling with Pt. The presence of brucite is confirmed by the detec-

tion of the stretching vibration at 3650 cm^{-1}. No other corrosion products have been identified.

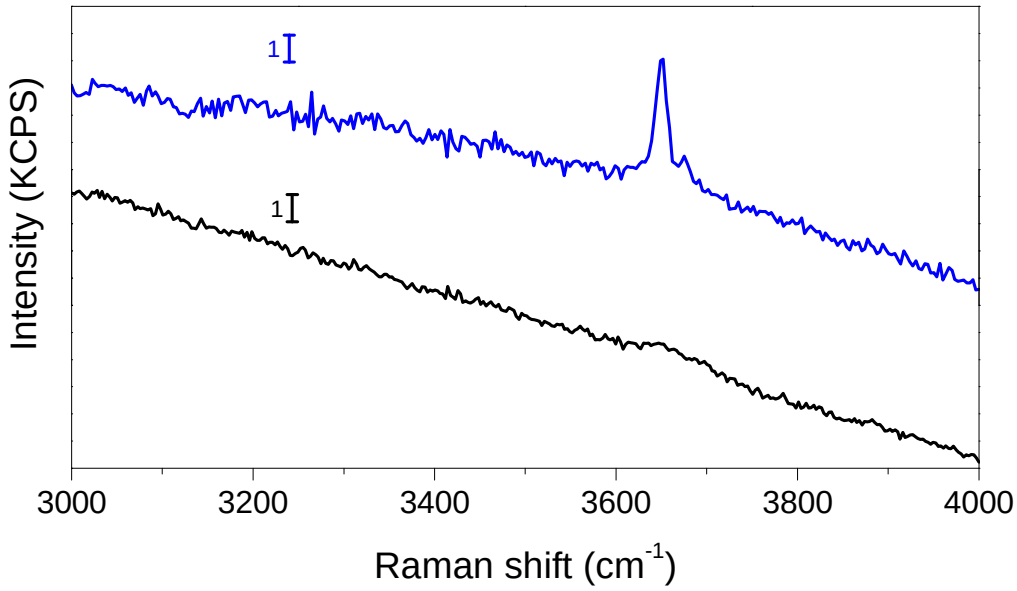

Figure 9: Raman spectra of Mg alloy before (in black) and after (in blue) galvanic coupling with Pt during 16h in 0.1M NaOH.

4 Conclusion

In this study, a protocol for sample preparation of Mg alloy and procedure for monitoring the values of potential and current with various galvanic coupling could be implemented. A classic basic solution of NaOH 0.1 M was chosen to perform the electrochemical measurements because it is the simplest case to reproduce pH of an interstitial solution of hydraulic binders in the case of encapsulation of Mg alloys. In this work, it was decided to carry out measurements in galvanic coupling with platinum, graphite and stainless steel 304L without prior stabilization of the Mg alloy in the electrolyte. The values of potential and current obtained indicate Butler-Volmer relationship, suggesting a cathodic control. The potential values of the galvanic coupling vary with the cathode, in ascending order for 304L, graphite and platinum. In view of these potential values, it was expected that the galvanic coupling leads to higher corrosion rates for platinum, graphite and 304L, respectively. However, 304L has a very high current density (and thus a higher corrosion) in comparison to that expected. Estimated corrosion rates vary from ten to several tens of micrometers per year.

It is important to remember that in the case of galvanic corrosion, the amount of hydrogen generated will be greater if the ratio between the cathode and the anode surface area is large, if the distance between these areas is small and if the conductivities of the electrolyte and the film surface is large. It was therefore selected for further studies, use of area ratios cathode / anode of about 10 /1 in a cell with a suitable geometry and performs measurements, always without any prior stabilization. This will place anodic control and maximize the corrosion of magnesium alloys. To better understand the phenomena involved, measurements of H_2 evolution and electrochemical impedance spectroscopy are also planned. Raman spectroscopy allows identifying brucite ($Mg(OH)_2$) as corrosion product.

5 References

[1] G.A. Fairhall, J.D. Palmer, The encapsulation of Magnox Swarf in cement in the United Kingdom, Cement and Concrete Research, 22 (1992) 293-298.
[2] D. Lambertin, F. Frizon, A. Blachere, F. Bart, Corrosion Behaviour of Mg Alloys in Various Basic Media: Application of Waste Encapsulation of Fuel Decanning from UNGG Nuclear Reactor, in: Magnesium Technology 2011, John Wiley & Sons, Inc., 2011, pp. 435-439.
[3] J. Morris, S. Wickham, P. Richardson, C. Rhodes, M. Newland, Asme, Contingency options for the drying, conditioning and packaging of Magnox spent fuel in the UK, 2010.
[4] A. Rooses, D. Lambertin, D. Chartier, F. Frizon, Galvanic corrosion of Mg–Zr fuel cladding and steel immobilized in Portland cement and geopolymer at early ages, Journal of Nuclear Materials, 435 (2013) 137-140.
[5] N.R. Smart, D.J. Blackwood, An investigation of the effect of galvanic coupling on the corrosion of container and waste metals in cementitious environments, AEAT-0251, issue C, in, 1998.
[6] G.G. Perrault, The potential-pH diagram of the magnesium-water system, Journal of Electroanalytical Chemistry and Interfacial Electrochemistry, 51 (1974) 107-119.
[7] M. Pourbaix, Atlas of Electrochemical Equilibria in Aqueous Solutions, National Association of Corrosion Engineers, 1974.
[8] G.L. Song, Corrosion of Magnesium Alloys, Woodhead Publishing, 2011.
[9] A. Atrens, W. Dietzel, The Negative Difference Effect and Unipositive Mg^{+}, Advanced Engineering Materials, 9 (2007) 292-297.
[10] D. Lambertin, F. Frizon, F. Bart, Mg-Zr alloy behavior in basic solutions and immobilization in Portland cement and Na-geopolymer with sodium fluoride inhibitor, Surface & Coatings Technology, 206 (2012) 4567-4573.
[11] P.M. Bradford, B. Case, G. Dearnaley, J.F. Turner, I.S. Woolsey, Ion beam analysis of corrosion films on a high magnesium alloy (Magnox Al 80), Corrosion Science, 16 (1976) 747-766.
[12] B. Weckler, H.D. Lutz, Near-infrared spectra of M(OH)Cl (M = Ca, Cd, Sr), Zn(OH)F, γ-$Cd(OH)_2$, $Sr(OH)_2$, and brucite-type hydroxides $M(OH)_2$ (M = Mg, Ca, Mn, Fe, Co, Ni, Cd), Spectrochimica Acta Part A: Molecular and Biomolecular Spectroscopy, 52 (1996) 1507-1513.